Fire retardant systems in poly(methyl methacrylate): interactions between metal oxide nanoparticles and phosphinates

Abdelghani Laachachi, Marianne Cochez, E. Leroy, Michel Ferriol, José-Marie Lopez-Cuesta

Fire retardant systems in poly(methyl methacrylate): Interactions between metal oxide nanoparticles and phosphinates

A. Laachachi [a], M. Cochez [a], E. Leroy [b], M. Ferriol [a,*], J.M. Lopez-Cuesta [b]

[a] *L.M.O.P.S., C.N.R.S. U.M.R. 7132, Université Paul Verlaine-Metz, BP 80105, rue Victor Demange, 57503 Saint-Avold Cedex, France*

[b] *Centre des Matériaux de Grande Diffusion, Ecole des Mines d'Alès, 6 avenue de Clavières, 30319 Alès Cedex, France*

In the course of our investigations on halogen-free fire-retardant solutions for PMMA, the influence of oxide nanoparticles (TiO_2, A $_2O_3$) o n the thermal stability and fire behaviour of PMMA blended with phosphinate additives (Exolit OP930 and OP1311) has been studied by thermogravimetric analysis and cone calorimetry. For each mixture, the residues obtained after combustion were examined and characterized by SEM, X-ray diffraction and X-ray microprobe analysis. Some synergistic effects were obtained between nanometric alumina and OP930 additive leading to the reduction of peak of heat released rate and of total heat released up to 30% and to the increase of time to ignition. From the results obtained, it can be proposed that OP930 and OP1311 act principally in the condensed phase, the presence of oxides playing a reinforcement role in the carbonaceous layer promoted by the phosphinate additives.

Keywords: PMMA, Poly(methyl methacrylate); Nanocomposites; Fire behaviour; Fire retardancy; Thermal stability; Phosphinates

1. Introduction

Over the last 10 years, various micro- or nanofillers have been shown to be efficient additives for improving the thermal stability and fire retardancy of various polymers [1,2]. Concerning poly(methyl methacrylate) (PMMA), numerous works have been published about the use of organo-modified clays [3−7], carbon nanotubes [7,8] and silica particles [9−16].

Our teams recently focussed on the use of metal oxide nanoparticles [17,18]. From our results, the role of metal oxide nanoparticles in the improvement of thermal stability [17] and flammability properties [18] was essentially attributed to the mobility restriction of polymer chains and to the thermal properties of the filler increasing the heat transfer inside the material which limits the ablation of the surface, the migration of gas bubbles and the release of combustible volatiles.

In a recent paper, we have reported on the existence of synergistic effects between alumina nanoparticles and ammonium polyphosphate (APP)-based additives [19] leading to an improvement of PMMA fire behaviour performance: higher ignition times, reduced heat release rate, reduced total heat released and significant increase of total burning time. To our knowledge, no similar data are available in the literature about the search for synergy between oxide nanoparticles and phosphorus fire retardants in PMMA. Nevertheless, similar synergistic effects have been found between nanofillers, such as clays, and conventional phosphorus fire retardants in styrenic polymers and poly(vinyl-esters) [20,21].

In order to promote halogen-free solutions for the PMMA fire retardancy and to get a better overview of the action of oxide nanoparticles with phosphorus-based additives, we have

* Corresponding author. Tel.: +33 3 87 93 91 85; fax: +33 3 87 93 91 01.
E-mail address: mferriol@univ-metz.fr (M. Ferriol).

Table 1
PMMA compositions containing OP930 and OP1311 additives and oxides

Composition (wt%)	PMMA	OP930	OP1311	Al_2O_3	TiO_2
PMMA	100	0	0	0	0
PMMA−15% Al_2O_3	85	0	0	15	0
PMMA−15% TiO_2	85	0	0	0	15
PMMA−15% OP930	85	15	0	0	0
PMMA−12% OP930−3% Al_2O_3	85	12	0	3	0
PMMA−9% OP930−6% Al_2O_3	85	9	0	6	0
PMMA−6% OP930−9% Al_2O_3	85	6	0	9	0
PMMA−3% OP930−12% Al_2O_3	85	3	0	12	0
PMMA−12% OP930−3% TiO_2	85	12	0	0	3
PMMA−9% OP930−6% TiO_2	85	9	0	0	6
PMMA−6% OP930−9% TiO_2	85	6	0	0	9
PMMA−3% OP930−12% TiO_2	85	3	0	0	12
PMMA−15% OP1311	85	0	15	0	0
PMMA−12% OP1311−3% Al_2O_3	85	0	12	3	0
PMMA−9% OP1311−6% Al_2O_3	85	0	9	6	0
PMMA−6% OP1311−9% Al_2O_3	85	0	6	9	0
PMMA−3% OP1311−12% Al_2O_3	85	0	3	12	0
PMMA−12% OP1311−3% TiO_2	85	0	12	0	3
PMMA−9% OP1311−6% TiO_2	85	0	9	0	6
PMMA−6% OP1311−9% TiO_2	85	0	6	0	9
PMMA−3% OP1311−12% TiO_2	85	0	3	0	12

chosen to investigate in the present work the influence of TiO_2 and Al_2O_3 on PMMA blended with phosphinate-based additives (Clariant Exolit OP930 and OP1311). These additives were selected for their effective fire retardant effects in oxygen-containing polymers such as polyamides and polyesters [22] and so, thought also to be efficient for PMMA.

2. Experimental

2.1. Materials

Poly(methyl methacrylate) (Oroglas, $M_w = 93\,000$ g mol^{-1}) was supplied by Atofina. Nanometric TiO_2 (P25) and Al_2O_3 (type C) were purchased from Degussa with respective median particle sizes equal to 21 and 13 nm and BET specific surface areas equal to 50 and 100 m^2 g^{-1}. Exolit OP930 and OP1311 additives were donated by Clariant GmbH.

X-ray diffraction and elemental analyses revealed that Exolit OP930 was a homogeneous crystalline metallic ethyl-phosphinate containing about 23 wt% of phosphorus with a median particle size of 3 μm. Exolit OP1311 was also a crystalline product, but SEM analysis showed aggregates of particles with sizes in the range 5−80 μm. Elemental analyses showed that OP1311 was also a metal ethyl-phosphinate enriched with nitrogenous compounds for synergistic effects. The element amounts were about 20 wt% for phosphorus and 14 wt% for nitrogen.

Table 2
Results of cone calorimeter experiments on PMMA−OP930 and PMMA−OP1311 blends

Compound	PMMA	PMMA−OP930 (15 wt%)	PMMA−OP1311 (15 wt%)
TTI (s)	69	70	35
TOF (s)	318	865	746
PHRR (kW m^{-2})	624	315	270
THR (MJ m^{-2})	112	91	73
TSR (m^2 m^{-2})	430	1797	1055
TCOR (g kg^{-1})	6.7	102.6	65.6

TTI: time to ignition; TOF: time of flameout; PHRR: peak of heat released rate; THR: total heat released; TSR: total smoke released; TCOR: total CO released.

2.2. Samples' preparation

All composite specimens were prepared by mixing molten PMMA pellets, nanoparticles and phosphorus additives in a Haake PolyLab 60 cm^3 mixer/rheometer at 225 °C and 50 rpm. An overall nanoparticles and additives percentage of 15% was selected to entail a significant effect on flame

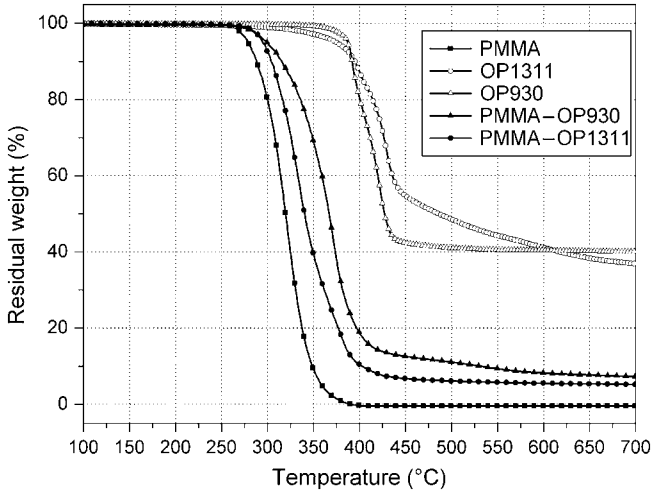

Fig. 1. TGA curves for thermo-oxidation of PMMA, OP930, OP1311 and their blends at 15 wt% in additive.

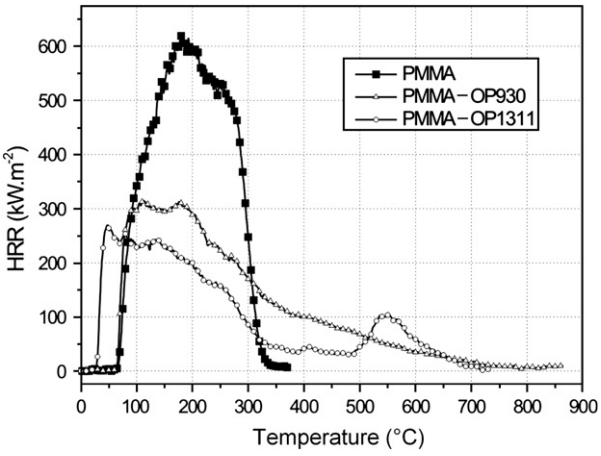

Fig. 2. Cone calorimetry of PMMA, PMMA−OP930 and PMMA−OP1311 blends: heat released rate curves (HRR) under an irradiation of 35 kW m^{-2}.

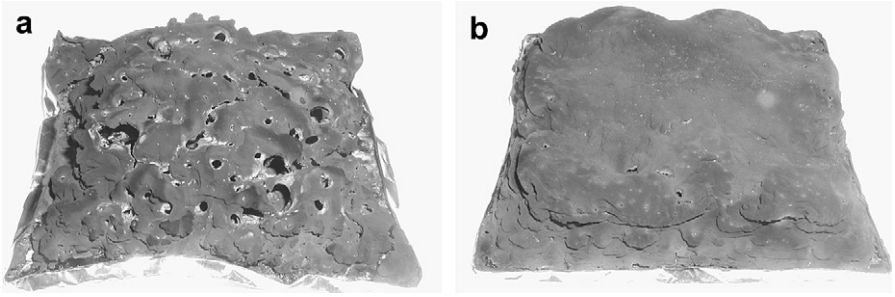

Fig. 3. Photographs of the residues obtained after combustion of mixtures PMMA−OP930 (a) and PMMA−OP1311 (b).

behaviour. Total mixing time was typically 7 min. Resulting composites were then pelletised using a rotary cutting mill before being compression moulded at 250 °C and 100 bar for 5 min in order to obtain $100 \times 100 \times 4$ mm^3 specimens. Table 1 presents the proportions in which oxides and OP additives were combined.

2.3. Experimental techniques

Thermogravimetric analyses (TGA) were performed with a Mettler-Toledo TGA/SDTA 851e thermobalance (horizontal balance mechanism), operating in air under a gas flow of 65 cm^3 min^{-1} with alumina crucibles (150 µl) containing 20−25 mg of sample. The runs were single ones and carried out in dynamic conditions at the constant heating rate of 10 °C min^{-1} on initial polymer compositions. The reproducibility of TGA measurements was confirmed with preliminary investigations on the thermal degradation of virgin PMMA for which duplicate measurements were performed at different heating rates (between 2 and 10 °C min^{-1}). The uncertainties on temperature and mass measurements were, respectively, estimated equal to 0.5 °C and 0.1 mg.

The evaluation of the flammability properties of PMMA and its composites was made using a cone calorimeter device (Fire Testing Technology). Sheets ($100 \times 100 \times 4$ mm^3) were exposed to the radiant cone (35 kW m^{-2}). The weight of samples was in the range 50−55 g. The heat release rate (HRR) was calculated from the oxygen consumption measured with a paramagnetic oxygen analyzer.

X-ray diffraction patterns were recorded at room temperature on a BRUKER D8 X-ray powder diffractometer fitted with a fast analyzer and using Cu Kα radiation.

SEM micrographs of cone calorimeter residues were made using an FEG environmental microscope (FEI-QUANTA type) equipped with an X-ray microprobe analysis device.

3. Results and discussion

3.1. PMMA−OP930 and PMMA−OP1311 blends

Fig. 1 gives the TGA curves of the two blends compared to pure PMMA and pure OP930 and OP1311. For both blends, the onset temperature (taken at 2% of mass loss) of 290 °C for OP930 and 283 °C for OP1311 is higher than that of pure PMMA (268 °C). On the whole, Fig. 1 shows that the thermal stability of blends is significantly improved and that the nitrogenous compounds contained in OP1311 are probably the cause of the lesser stability of this blend. A residue of about 5% of the initial mass is observed for the two blends. Taking into account the weight content of additives in the blends, this roughly corresponds to the residue obtained for each additive alone.

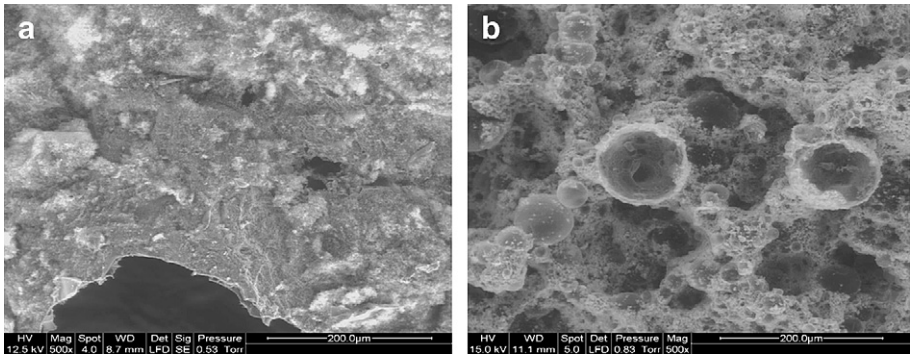

Fig. 4. SEM photographs of the residues obtained after combustion of PMMA−OP930 (a) and PMMA−OP1311 (b) blends (magnification: ×500).

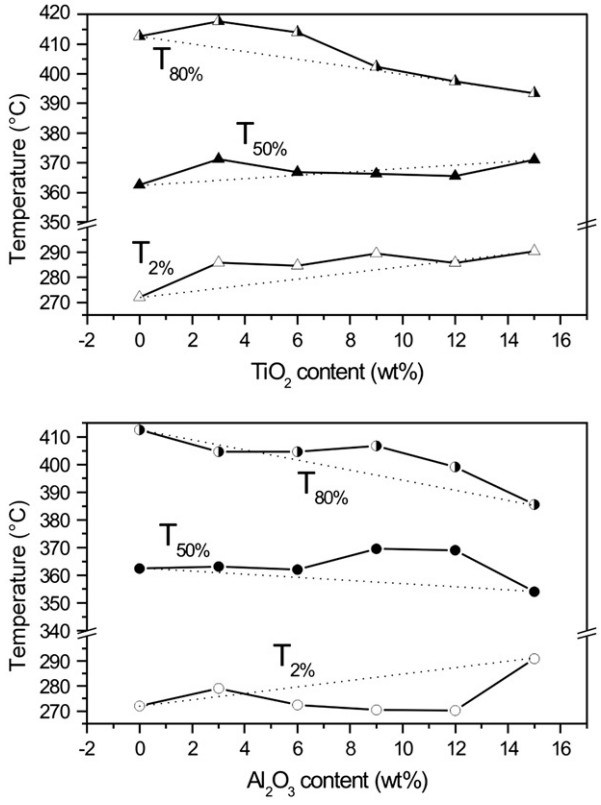

Fig. 5. Influence of the oxide content on the thermal stability of PMMA−OP930 mixtures for a total loading for additives of 15 wt%: summary of results.

Fig. 7. Photograph of the residue obtained after combustion of the mixture PMMA−9% OP930−6% Al_2O_3.

Table 2 and Fig. 2 present the results of cone calorimeter experiments. For OP930, the time to ignition (TTI) remains unchanged and is decreased by 50% for OP1311. This reduction could be caused by the easy ignition of the decomposition products of the nitrogenous compounds contained in OP1311 and not involved in OP930. However, a significant reduction

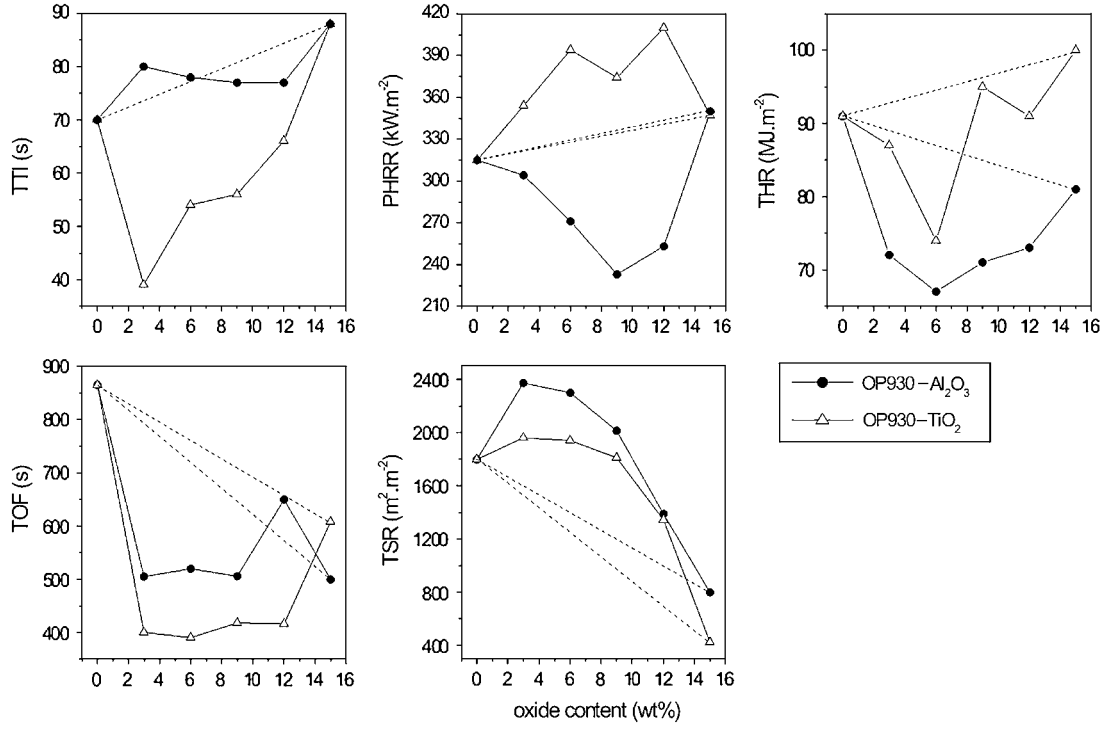

Fig. 6. Influence of the oxide content on the major parameters measured during cone calorimetry experiments for PMMA−OP930 mixtures (total loading for additives: 15 wt%).

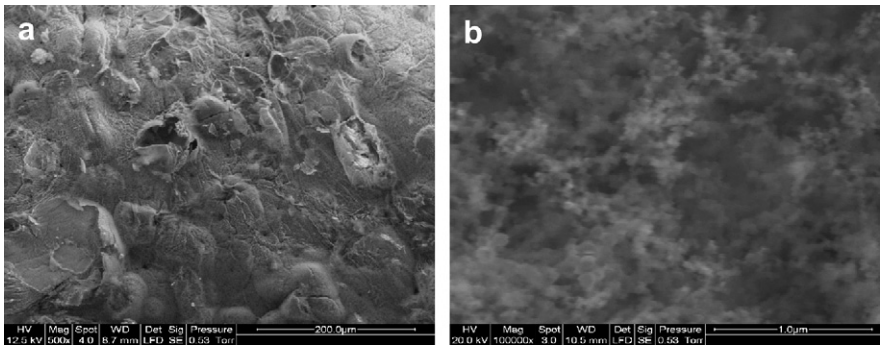

Fig. 8. SEM photographs of the residue obtained after combustion of the mixture PMMA−9% OP930−6% Al_2O_3 (magnification: (a) ×500, (b) ×100 000).

in heat release rate is observed as shown by PHRR decreased by 50% or more. But the production of smoke and CO is dramatically increased, signs of an incomplete combustion. These results indicate a probable modification of the PMMA decomposition pathway since, for OP1311, a residue is formed with an amount higher than the initial quantity of additive, showing the participation of PMMA degradation products to the formation of the residue.

Fig. 3 shows the photos of the residues obtained after cone calorimeter tests. An expanded carbonaceous layer (with some holes in the case of OP930) can be seen which protects the material against heat flux and reduces the evaporation rate of degradation gases and therefore, the degradation rate of the sample. This is confirmed by the increase of the time of flameout (TOF) (Table 2). X-ray diffractograms evidenced the vitreous state of the formed layer and X-ray microprobe analysis showed the presence of phosphorus, oxygen, carbon and aluminium. Observed by SEM (Fig. 4), the layer obtained with OP930 appeared compact and homogeneous although the presence of cracks suggested poor mechanical resistance. For OP1311, a brittle porous residue with spherical alveolar particles was observed (Fig. 4).

These results show a positive influence of OP930 and OP1311 additives on the thermo-oxidative degradation and reaction to fire of PMMA.

Fig. 9. Photograph of the residue obtained after combustion of the mixture PMMA−9% OP930−6% TiO_2.

3.2. PMMA−OP930−Al_2O_3 and PMMA−OP930−TiO_2 composites

3.2.1. Thermal stability

Fig. 5 gives the evolution of beginning ($T_{2\%}$), half ($T_{50\%}$) and ending ($T_{80\%}$) degradation temperatures recorded during TGA experiments for the different compositions in TiO_2 and Al_2O_3 investigated (Table 1).

With TiO_2, below 9 wt%, a stabilizing effect (degradation temperature above the one given by an additive law as a function of the substitution amount of OP930 by oxide) can be seen suggesting some synergism at the different stages of the degradation pathway. From about 9−10 wt%, the three temperatures increase, practically following a linear additive law signifying the absence of a particular effect. On the whole, Fig. 5 shows the stabilizing effect of titanium oxide attributed to the mobility restriction of the polymer chains (steric hindrance and surface adsorption on the oxide particles) as previously shown [1−3].

With Al_2O_3, up to about 6 wt%, the evolution of $T_{2\%}$, $T_{50\%}$ and $T_{80\%}$ follows a linear additive law showing that no particular effect is caused by the substitution of OP930 by alumina. Above 6 wt%, the evolution of $T_{50\%}$ and $T_{80\%}$ suggests some synergism and increased stability (by comparison to the additive law) for the intermediate compositions with 9 and 12 wt% Al_2O_3. The evolution of the onset temperature ($T_{2\%}$) would show, on the contrary, a catalytic effect of alumina−OP930 blends on the degradation (antagonism) for the same range of compositions. The stabilizing effect of alumina by an increased mobility restriction of the polymer chains can also be invoked to explain the

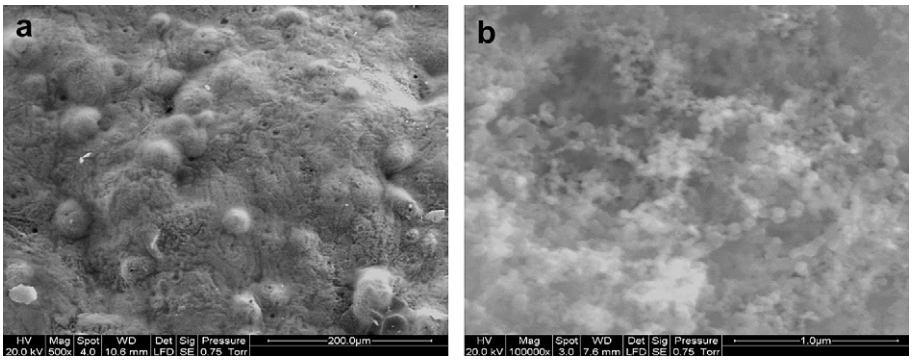

Fig. 10. SEM photographs of the residue obtained after combustion of the mixture PMMA−9% OP930−6% TiO_2 (magnification: (a) ×500, (b) ×100 000).

synergistic effect between alumina and the phosphinate additive.

3.2.2. Cone calorimetry

The results of the cone calorimeter experiments are summarized in Fig. 6. They show that the partial substitution of OP930 by alumina nanoparticles leads to the improvement of the fire behaviour: increasing time to ignition (TTI), peak of heat release rate (PHRR) and total heat released (THR) with synergistic effects on both PHRR and THR. However, the time of flameout (TOF) and the total smoke released (TSR) show a rather marked antagonism. With TiO_2, no significant improvement is achieved except, perhaps, for THR.

The visual observation of the residues involving alumina shows essentially a continuous solid layer as typically illustrated in the case of the sample PMMA−9% OP930−6% Al_2O_3 (Fig. 7). When the oxide content increases, the layer is less expanded and the density of cracks at its surface increases. SEM observations show the existence of a cohesive structure with nodules (Fig. 8(a)) and that the alumina particles are well dispersed in the material (Fig. 8(b)) as confirmed by X-ray microanalysis which also indicated the presence of P, O, C and Al chemical elements. X-ray diffraction experiments on the residues confirmed the presence of Al_2O_3 as the only one crystalline compound. It can be concluded that no chemical reaction occurred between alumina and OP930 and that a vitreous layer was formed promoted by the phosphorated compound and reinforced by alumina particles.

With the same amounts of TiO_2, the charred residue does not cover the entire surface initially occupied by the sample (Fig. 9) leading to a poor barrier effect, which explains the less good results obtained in this case (TTI, PHRR for instance). SEM observations confirmed the good dispersion of TiO_2 and that, when existing, the char formed a cohesive structure showing nodules as for Al_2O_3 (Fig. 10). The absence of crystalline compounds other than TiO_2 (anatase and rutile phases corresponding to the starting compound) was found by X-ray diffraction whereas X-ray microprobe showed that the charred vitreous layer contained P, O, C, Ti and Al elements.

As a conclusion, it appears that beyond their role of char reinforcement, alumina particles have a positive catalytic effect on the formation of the protective layer with OP930 additive not provided by titanium oxide particles.

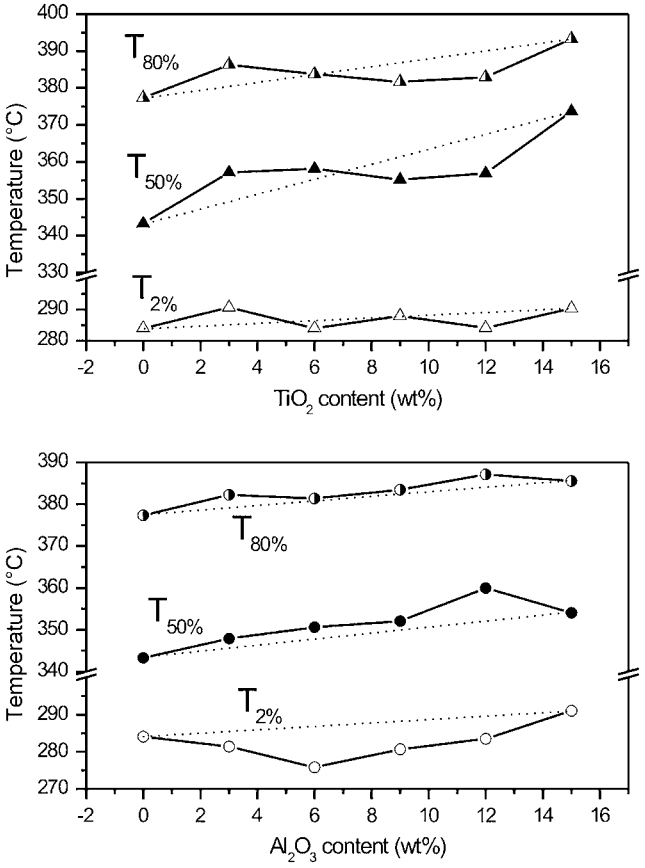

Fig. 11. Influence of the oxide content on the thermal stability of PMMA−OP1311 mixtures for a total loading for additives of 15 wt%: summary of results.

3.3. PMMA−OP1311−Al_2O_3 and PMMA−OP1311−TiO_2 composites

3.3.1. Thermal stability

As for OP930, Fig. 11 gives the evolution of $T_{2\%}$, $T_{50\%}$ and $T_{80\%}$ for TiO_2 containing samples. In the three cases, we can

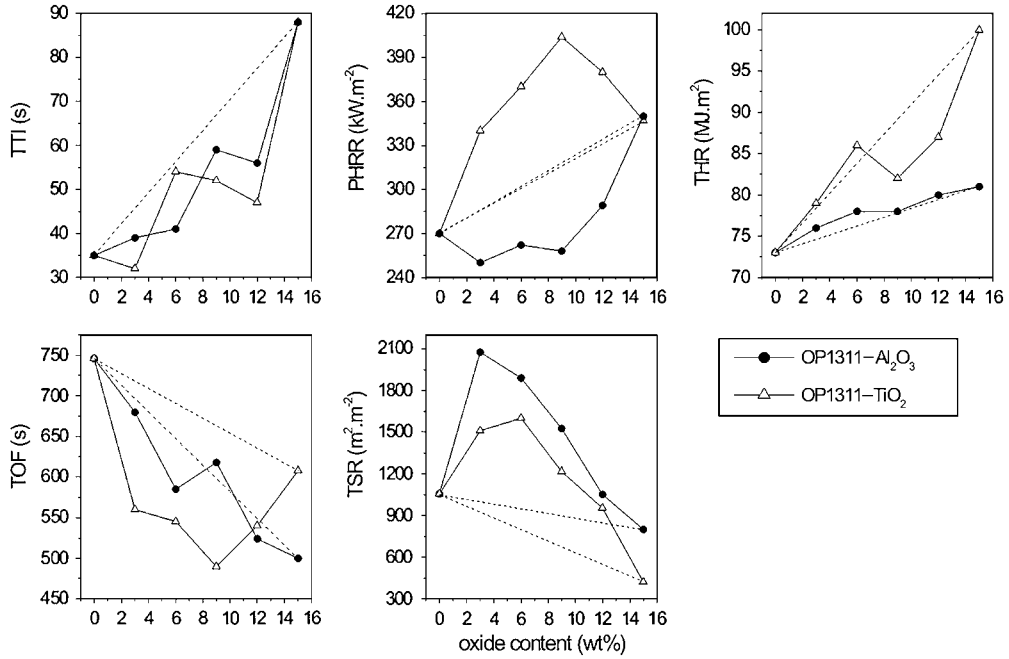

Fig. 12. Influence of the oxide content on the major parameters measured during cone calorimetry experiments for PMMA−OP1311 mixtures (total loading for additives: 15 wt%).

note the same stabilizing effect as for OP930 up to 5 wt% and a catalytic effect from about 7 to 8 wt% (rather than a neutral effect for OP930), apparently more marked in the late stages of the degradation (from 50%).

For Al_2O_3, $T_{2\%}$ evolves in the same way than with OP930. For $T_{50\%}$ and $T_{80\%}$, the evolution of the degradation temperature shows that synergistic effects above 8 wt% are less important than for OP930.

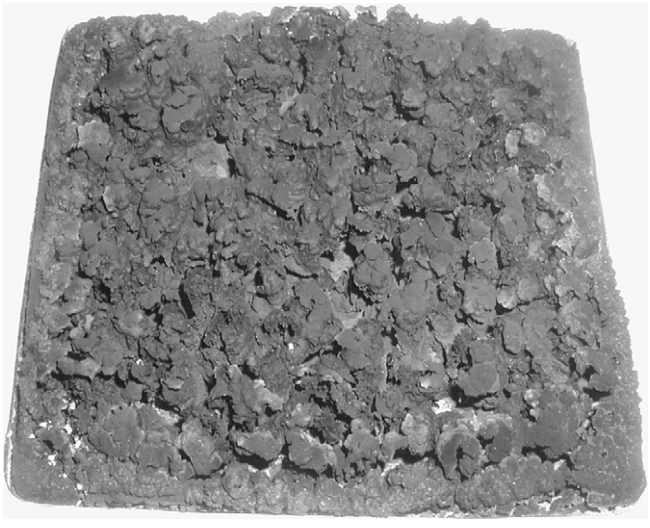

Fig. 13. Photograph of the residue obtained after combustion of the mixture PMMA−6% OP1311−9% Al_2O_3.

Globally, the comparison of OP930 and OP1311 allows us to confirm that the nitrogenous compounds contained in OP1311 contribute to a loss of stability of PMMA even in the case of mixtures with TiO_2 and Al_2O_3.

3.3.2. Cone calorimetry

Fig. 12 gives an overview of the results obtained. On the whole, they are similar to those obtained with OP930 but, for the two oxides, the synergisms and antagonisms are less marked. Al_2O_3 appears to be more efficient than TiO_2 as for OP930.

For alumina, the visual observation of residues shows that the expanded carbonaceous layer obtained with only OP1311 (Fig. 3(b)) is more and more cracked when the amount of oxide increases. This limits its expansion as illustrated, for example, by Fig. 13 giving the photograph of the residue obtained for the composition PMMA−6% OP1311−9% Al_2O_3. Under SEM, the residues show a cohesive structure with nodules and a good dispersion of oxide particles. From 9 wt% Al_2O_3, holes can be observed (Fig. 14). The structural analysis of the residues by X-ray diffraction confirmed both the vitreous state observed with additive alone and the presence of only Al_2O_3 crystals confirming the absence of chemical reaction between alumina particles and OP1311 leading to a crystalline structure. Thus, the vitreous layer appears reinforced by nanometric alumina particles.

With TiO_2, in contrast to the observations made with OP930, the carbonaceous layer covers all the surface of the

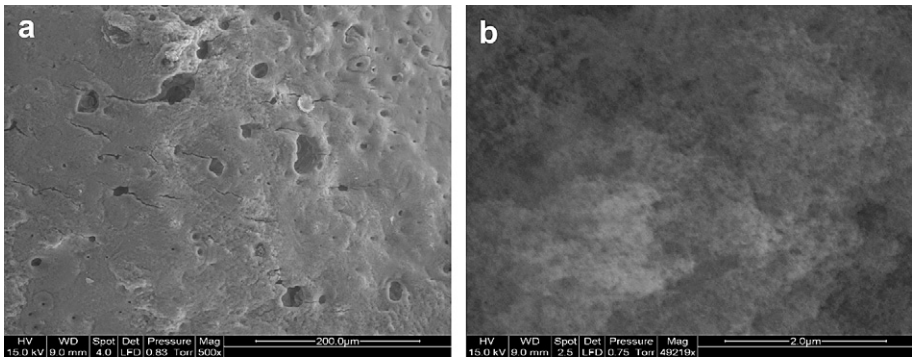

Fig. 14. SEM photographs of the residue obtained after combustion of the mixture PMMA−6% OP1311−9% Al_2O_3 (magnification: (a) ×500, (b) ×50 000).

sample. When the amount of oxide increases, the same cracking phenomenon of the carbonaceous layer, seen with alumina, is observed (Fig. 15) and the expansion of the layer is then less than with OP1311 alone. As an example, the SEM photographs of the residue corresponding to the composition PMMA−6% OP1311−9% TiO_2 (Fig. 16) show a cohesive structure with some porosity leading to some brittleness which is not observed with alumina. X-ray diffraction confirmed the vitreous character of the carbonaceous layer and that no chemical reaction leading to a crystalline structure occurred between OP1311 and TiO_2 (crystalline phases observed: anatase and rutile as for the starting oxide). Ti, Al, O, C and P chemical elements were identified by microprobe analysis.

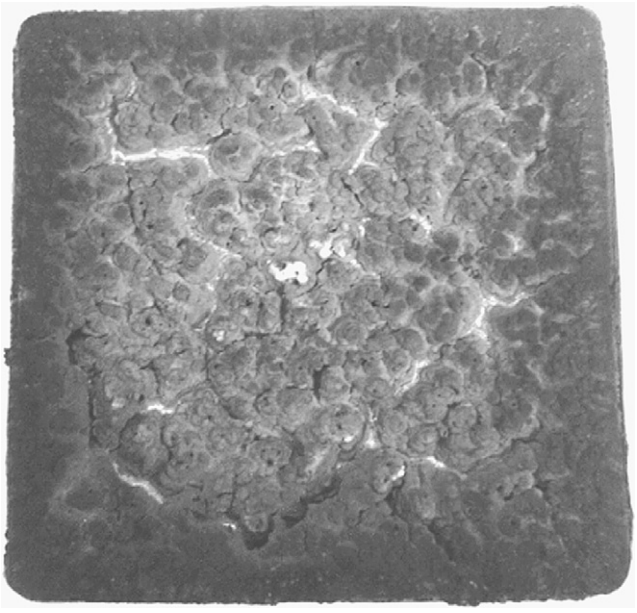

Fig. 15. Photograph of the residue obtained after combustion of the mixture PMMA−6% OP1311−9% TiO_2.

Compared to alumina, the lower fire performances observed with TiO_2 can be largely ascribed to the lower compactness and apparently poorer mechanical behaviour of the carbonaceous layer.

The comparison of the results obtained during this work with literature data involving other kinds of polymers, nanoparticles and phosphorus fire retardants can only be tentative because of their different chemical nature. Moreover, in most cases, their concentration is not the same and only the value of PHRR is given. If the diminution of PHRR is an important factor in fire retardancy, other parameters have to be taken into account: TSR, TOF, TTI, … to allow reliable comparisons. However, in this work, the best results were obtained with the 9% Al_2O_3−6% OP930 combination for which PHRR decreases by about 30% and THR by about 25% towards virgin PMMA which is comparable to values obtained with other systems in a similar concentration range (for example: 40−50% for the reduction of PHRR and 15−30% for THR in PVE with clay and phosphates [21]).

4. Conclusions

The combination of phosphinate additives with metal oxide nanoparticles such as Al_2O_3 or TiO_2 can enhance the thermal stability and fire behaviour of PMMA. All the results obtained tend to indicate that the phosphinate additives studied act principally in the condensed phase, the presence of oxides playing a reinforcement role for the carbonaceous layer promoted by the phosphinate additives. However, TiO_2 does not improve the fire behaviour of the composites significantly enough whatever may be the phosphinate additive used. With Al_2O_3, interesting results were obtained with OP930 justifying a further investigation of the intimate mechanism of the fire-retardant action of metallic phosphinates and of their interaction with oxide nanoparticles which, despite high activity in industrial laboratories, are not fundamentally studied in academic laboratories nowadays. This work is in progress.

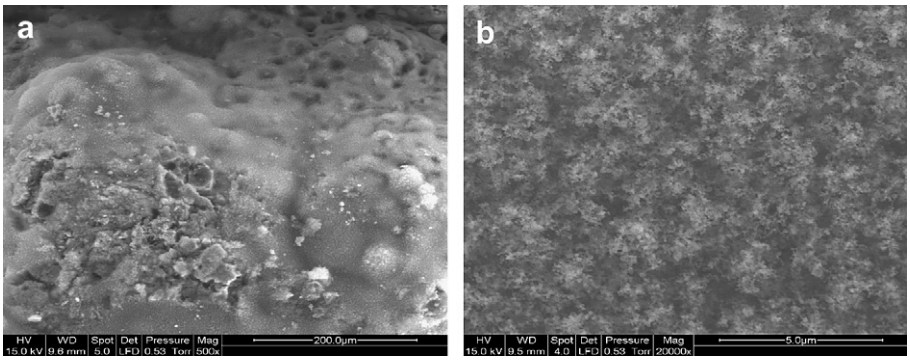

Fig. 16. SEM photographs of the residue obtained after combustion of the mixture PMMA−6% OP1311−9% TiO_2 (magnification: (a) ×500, (b) ×20 000).

References

[1] Bourbigot S, Duquesne S, Jama C. Macromol Symp 2006;233:180.
[2] Beyer G. Polym Polym Comp 2005;13:529.
[3] Gilman JW. Appl Clay Sci 1999;15:31.
[4] Su S, Jiang DD, Wilkie CA. Polym Adv Technol 2004;15:225.
[5] Zhu J, Start P, Mauritz KA, Wilkie CA. Polym Degrad Stab 2002;77:253.
[6] Kumar S, Jog JP, Natarajan U. J Appl Polym Sci 2003;89:1186.
[7] Costache MC, Wang D, Heidecker MJ, Manias E, Wilkie CA. Polym Adv Technol 2006;17:272.
[8] Kashiwagi T, Du F, Douglas JF, Winey KI, Harris Jr RH, Shields JR. Nature Mater 2005;4:928.
[9] Gilman JW, Ritchie SJ, Kashiwagi T, Lomakin SM. Fire Mater 1997;21:23.
[10] Chang TC, Wang YT, Hong YS, Chiu YS. J Polym Sci Part A 2000;38:1972.
[11] Kashiwagi T, Shields JR, Harris Jr RH, Davis R. J Appl Polym Sci 2003;87:1541.
[12] Kashiwagi T, Morgan AB, Antonucci JM, Vanlandingam MR, Harris Jr RH, Awad WH, et al. J Appl Polym Sci 2003;89:2072.
[13] Feng Y, Gordon NL. J Appl Polym Sci 2004;89:3844.
[14] Yu-Hsiang H, Chuh-Yung C, Cheng-Chien W. Polym Degrad Stab 2004;84:545.
[15] Aruchamy A, Blackmore KA, Zelinski BJJ, Uhlmanm DR, Booth C. Mater Res Soc Symp Proc 1992;249:353.
[16] Morgan AB, Antonucci JM, Vanlandingham MR, Harris RH, Kashiwagi T. Polym Mater Sci Eng 2000;83:57.
[17] Laachachi A, Cochez M, Ferriol M, Lopez-Cuesta JM, Leroy E. Mater Lett 2005;59:36.
[18] Laachachi A, Leroy E, Cochez M, Ferriol M, Lopez-Cuesta JM. Polym Degrad Stab 2005;89:344.
[19] Laachachi A, Cochez M, Leroy E, Gaudon P, Ferriol M, Lopez-Cuesta JM. Polym Adv Technol 2006;17:327.
[20] Chigwada G, Wilkie CA. Polym Degrad Stab 2003;81:551.
[21] Chigwada G, Panchatapa J, Jiang DD, Wilkie CA. Polym Degrad Stab 2005;89:85.
[22] Levchik S, Weil ED. Polym Int 2005;54:11.